GPS Solutions (2021) 25:15
https://doi.org/10.1007/s10291-020-01048-0

ORIGINAL ARTICLE

# Impact of robot antenna calibration on dual-frequency smartphone-based high-accuracy positioning: a case study using the Huawei Mate20X

**Francesco Darugna[1,2] · Jannes B. Wübbena[1] · Gerhard Wübbena[1] · Martin Schmitz[1] · Steffen Schön[2] · André Warneke[1]**

Received: 8 June 2020 / Accepted: 15 October 2020 / Published online: 10 November 2020


## Abstract

The access to Android-based Global Navigation Satellite Systems (GNSS) raw measurements has become a strong motivation to investigate the feasibility of smartphone-based positioning. Since the beginning of this research, the smartphone GNSS antenna has been recognized as one of the main limitations. Besides multipath (MP), the radiation pattern of the antenna is the main site-dependent error source of GNSS observations. An absolute antenna calibration has been performed for the dual-frequency Huawei Mate20X. Antenna phase center offset (PCO) and variations (PCV) have been estimated to correct for antenna impact on the L1 and L5 phase observations. Accordingly, we show the relevance of considering the individual PCO and PCV for the two frequencies. The PCV patterns indicate absolute values up to 2 cm and 4 cm for L1 and L5, respectively. The impact of antenna corrections has been assessed in different multipath environments using a high-accuracy positioning algorithm employing an undifferenced observation model and applying ambiguity resolution. Successful ambiguity resolution is shown for a smartphone placed in a low multipath environment on the ground of a soccer field. For a rooftop open-sky test case with large multipath, ambiguity resolution was successful in 19 out of 35 data sets. Overall, the antenna calibration is demonstrated being an asset for smartphone-based positioning with ambiguity resolution, showing cm-level 2D root mean square error (RMSE).

**Keywords** Absolute robot antenna calibration · GNSS · Smartphone-based high-accuracy positioning

## Introduction

The Global Navigation Satellite System (GNSS) antenna quality is a crucial factor in smartphone-based positioning. The use of an omnidirectional linearly polarized antenna in mobile devices has advantages in terms of received signal strength and the number of received signals (Pathak et al. 2003), but also makes the antenna very sensitive to multipath (MP) effects. This is generally accepted since the design drivers of smartphone antennas (e.g., continuous signal reception in any location) lead to seeking the highest sensitivity. Moreover, the smartphone antenna is affected by the other components of these portable devices, e.g., the screen of the cell phone (Xiao et al. 2019). The high levels of non-suppressed local MP cause significant and hard to predict phase errors, making ambiguity resolution even more challenging, as pointed out by Pesyna Jr et al. (2014) and Humphreys et al. (2016). Smartphone-based high-accuracy

✉ Francesco Darugna
francesco.darugna@geopp.de

Jannes B. Wübbena
jannes.wuebbena@geopp.de

Gerhard Wübbena
gerhard.wuebbena@geopp.de

Martin Schmitz
martin.schmitz@geopp.de

Steffen Schön
schoen@ife.uni-hannover.de

André Warneke
andre.warneke@geopp.de

[1] Geo++ GmbH, Steinriede 8, 30827 Garbsen, Germany

[2] Institut für Erdmessung, Schneiderberg 50, 30167 Hannover, Germany

positioning is therefore challenging, but several studies suggest that, under some pre-requisites, it is feasible.

Multiple authors investigated the quality of smartphone GNSS measurements (Massarweh et al. 2019) and developed strategies to improve positioning results in precise point positioning (PPP) type solutions without ambiguity resolution (Zhang et al. 2018; Wu et al. 2019).

Various research groups investigated the potential of ambiguity resolution with a smartphone receiver, using an external GNSS antenna. Humphreys et al. (2016) suggested that smartphones seem to be fully capable of supporting cm-accurate carrier-phase differential GNSS positioning when placed in appropriate locations. For example, Geng and Li (2019) show that with a Xiaomi Mi8 smartphone coupled with an external antenna, it is possible to obtain a reliable ambiguity-fixed solution.

A different approach to achieve ambiguity resolution with smartphones is to directly use the smartphone antenna but employ the phone in specifically designed test cases with highly reduced multipath. Darugna et al. (2019) demonstrated that ambiguity resolution is indeed possible with smartphones when used with a choke ring type of ground plane on a moving platform. Bochkati et al. (2020) show comparable results when the smartphone is undergoing a slow circular motion.

The site-dependent effects of GNSS measurements are only partly due to reflections in the vicinity of the antenna. Another contribution is the signal reception in the antenna itself. In the case of phase observations, these distortions are called phase center variations (PCV) and refer to a mean center, an imaginary point thought of as the point where the signals are on average received. This center does typically not align with the antenna reference point (ARP), which is a well-defined point accessible from outside the antenna. The mean phase center and the geometric offset to the ARP define the so-called phase center offset (PCO), which is the vector between ARP and mean phase center, pointing toward the mean phase center. Here, we report on the PCV computed for L1 and L5 frequencies derived from a common adjustment of GPS and Galileo observations. Nowadays, high precision applications require mm-level PCV for the most extensive elevation range possible (Teunissen and Montenbruck, 2017). The full description of the phase behavior is called antenna correction, and the procedure to determine PCO and PCV is called antenna calibration. During the years, many working groups developed antenna calibration techniques, e.g., anechoic chamber measurements (Schupler et al. 1994), relative field calibrations (Rothacher et al. 1995; Mader 1999), and absolute field calibrations (Wübbena et al. 1997, 2000; Menge 2003; Kersten 2014, Willi 2019). A comparison between the chamber and absolute field calibrations can be found in Görres et al. (2006) and Willi et al. (2020).

To our knowledge, no attempt to perform an absolute antenna calibration for a smartphone has yet been published. Netthonglang et al. (2019) computed an approximated antenna phase center of the Xiaomi Mi8 smartphone by averaging the post-processing coordinates in northing and easting. Their study showed centimeter-level relative positioning using roughly 5 and 20 km baselines after mainly removing the multipath effects. Wanninger and Heßelbarth (2020) presented results of a relative calibration of the L1 frequency of a Huawei P30 with respect to a geodetic reference antenna. With the calibration, they were able to achieve 2 cm-accurate positioning after 60 min of convergence.

Here, we perform an absolute, multi-frequency antenna calibration exemplarily for a Huawei Mate20X phone. We employ the robot-based absolute antenna field calibration (Wübbena et al. 1997, Wübbena et al. 2000, Schmitz et al. 2002, Rothacher 2001) to retrieve PCO and PCV corrections. These parameters are demonstrated to be an asset to smartphone-based positioning. The impact of antenna corrections on the positioning performance is investigated, and the outcome is reported. In the first section, we present the robot antenna calibration concept, along with the PCV description. Successively, we discuss the resulting PCV pattern. In the following section, the positioning results are reported after applying the antenna corrections, showing high-accuracy positioning with fixed ambiguities in open sky environments. Finally, we summarize the main conclusions and suggest possible future work.

## Absolute robot-based field calibration of GNSS antennas

PCV are not homogenous in space. They can be expressed as a function of two angles: azimuth $\alpha$ and zenith $\theta$. As presented in Rothacher et al. (1995), such a function can be expanded with spherical harmonics. Accordingly, the PCV can be described as:

$$PCV(\alpha,\theta) = \sum_{n=0}^{n_{\max}} \sum_{m=0}^{n} [A_{nm}\cos(m\alpha) + B_{nm}\sin(m\alpha)]P_{nm}\cos(\theta). \quad (1)$$

In Eq. 1, $\alpha$ and $\theta$ refer to the position of a specific satellite in the antenna coordinate system, $P_{nm}$ are the fully normalized Legendre polynomials, and $A_{nm}$ and $B_{nm}$ are the coefficients estimated for maximum degree $n_{\max}$ and maximum order $m_{\max} \leq n_{\max}$.

It is worth observing that the PCV depend on the frequency of the received signal, being independent of the GNSS involved (here, GPS and Galileo). Therefore, the results are the same for L1-E1 and L5-E5a and here reported equivalently.

The antenna calibration provides the antenna corrections, i.e., PCO and PCV, applied to the positioning algorithm. Since in a GNSS observation equation, the effect of the two sources of station dependent errors cannot be distinguished, the determination of PCV or MP requires the elimination or separation of one of the two (Schmitz et al. 2002). The rapid movement of the robot used in robot antenna calibration causes a change in the antenna orientation (rotations, tilts), introducing a variation of only the PCV every epoch, thus allowing the separation between antenna errors and multipath. This effect is taken into account in the Kalman filter process, where the residual multipath is estimated as a stochastic process with a correlation length of 60 s (Wübbena et al. 2000), allowing to assess the antenna phase variation through fast orientation changes. Several thousands of robot positions are evaluated through the tilts and rotations, allowing to define the shape of the PCV. The azimuth- and elevation-dependent PCV are described by a spherical harmonic expansion (see (1)). We used spherical harmonics of degree eight and order five. Moreover, the PCV are centered to zero for zenith angles equal to zero, i.e., $PCV(\theta = 0) = 0$. We refer to Wübbena et al. (1997), Wübbena et al. (2000) and Schmitz et al. (2002) for further details about the concept of the robot-based absolute antenna calibration.

Figure 1 shows the setup for the antenna calibration of the smartphone and the simplified dataflow to estimate the antenna corrections. The Mate20X was mounted on the robot, aligning the geometrical center of the smartphone with the rotational center of the robot. In this case, the rotational center corresponds to the ARP. The smartphone's observations acquired during the calibration have been post-processed in a multi-frequency GNSS antenna calibration along with GNSS observations from a geodetic reference station.

At the end of the process, antenna corrections in the ANTEX format (Rothacher and Schmid, 2010) are generated to describe the elevation- and azimuth-dependent PCV completely. In the following paragraph, the results of the calibration are applied in smartphone positioning.

## Analysis of smartphone's PCV

The magnitude of the PCV is shown in Figs. 2 and 3 for L1 and L5 frequency, respectively. PCV magnitudes up to about 2 cm and 4 cm are observed for L1 and L5, respectively, with formal STDs (1 $\sigma$) lower than 1.6 mm. These STDs are related to the variance–covariance matrix of the whole state estimation process. Consequently, they are affected by both the estimation of the parameters of the spherical harmonics and the quality of the observations. The variations over azimuth and elevation of the magnitude of the estimated PCV values are 7 mm and 10 mm for L1 and L5 frequencies. The Mate20X PCV are larger than those of a typical rover antenna that shows typically PCV lower than 10 mm, with a variation smaller than 2 mm. The largest magnitudes of the PCV occur for azimuthal angles $\alpha \in [270°, 360°[$ for the L1 frequency (see Fig. 2) and for $\alpha \in [230°, 360°[$ for the L5 frequency (Fig. 3). Comparing Figs. 2, 3, and 4, it can be observed that the largest absolute values of PCV are in directions of the major part of the smartphone's body with respect to the antenna phase center locations. The smartphone components (housing and active electronics), as well as near field effects in that direction, might affect the signal reception resulting in larger PCV.

Twelve distinct antenna calibrations have been carried out with the Mate20X to assess the repeatability of the absolute PCV. A single antenna calibration duration goes from a minimum of six hours to a maximum of 37 h. As an example, Fig. 5 and 6 show the magnitude of the difference

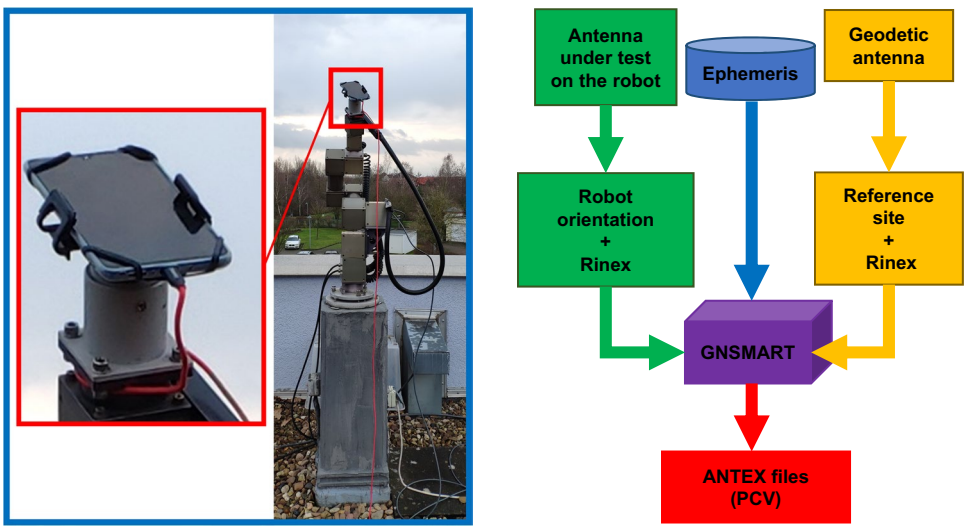


**Fig. 1** From left to right: robot antenna calibration setup and simplified processing scheme of the calibration of the smartphone antenna. The Mate20X was carefully mounted, allowing the device to be continuously charged

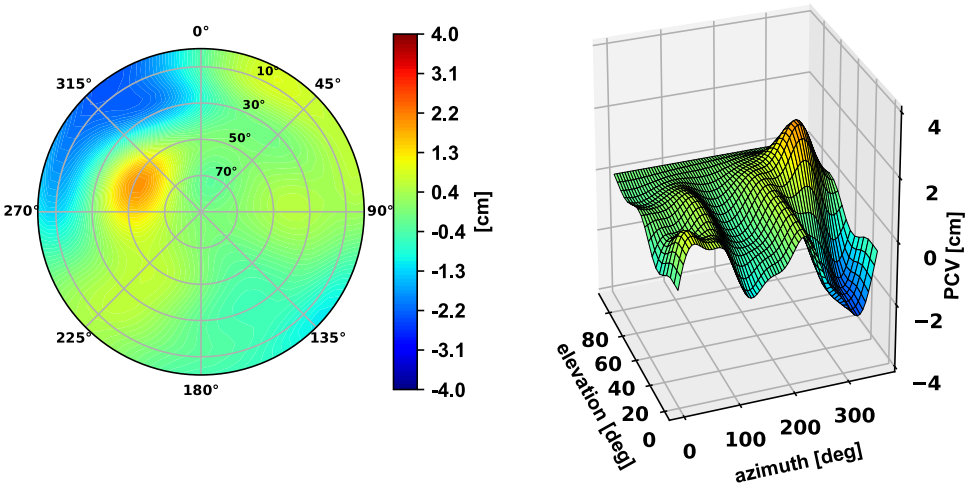


**Fig. 2** L1 PCV of the Mate20X smartphone antenna. Polar and 3D plot with respect to azimuth and elevation are reported

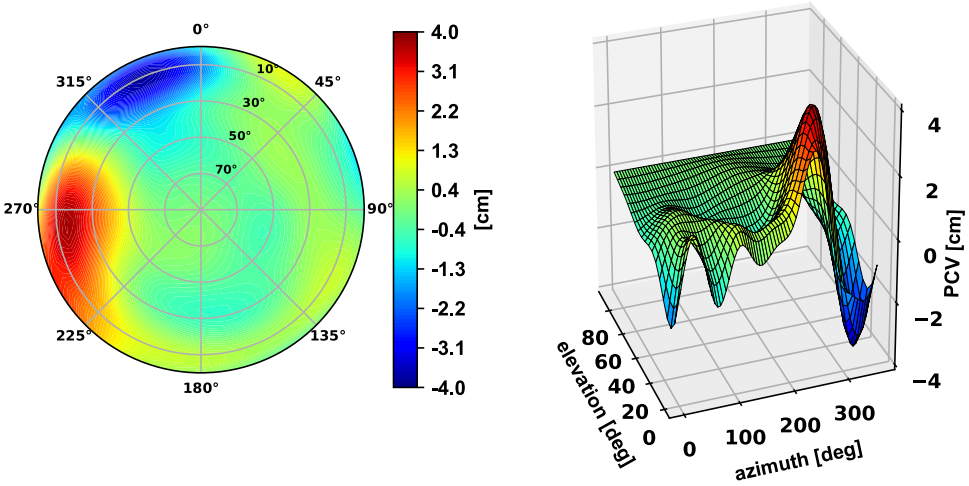


**Fig. 3** L5 PCV of the Mate20X smartphone antenna. Polar and 3D plot with respect to azimuth and elevation are reported

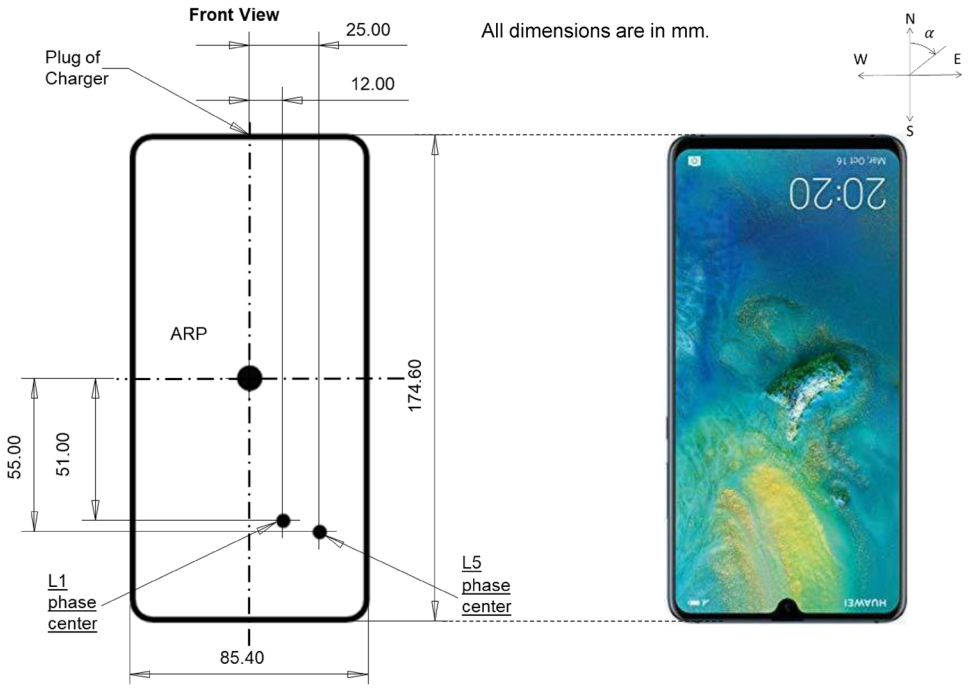


**Fig. 4** Location of the estimated phase centers for L1 and L5 frequencies within the Mate20X and the north definition of the antenna calibration. The larger magnitudes of PCV depicted in Figs. 2 and 3 are in correspondence of the opposite corner of the antenna phase center locations. All the dimensions are reported in mm. The plug of the charger is defined as the NRP

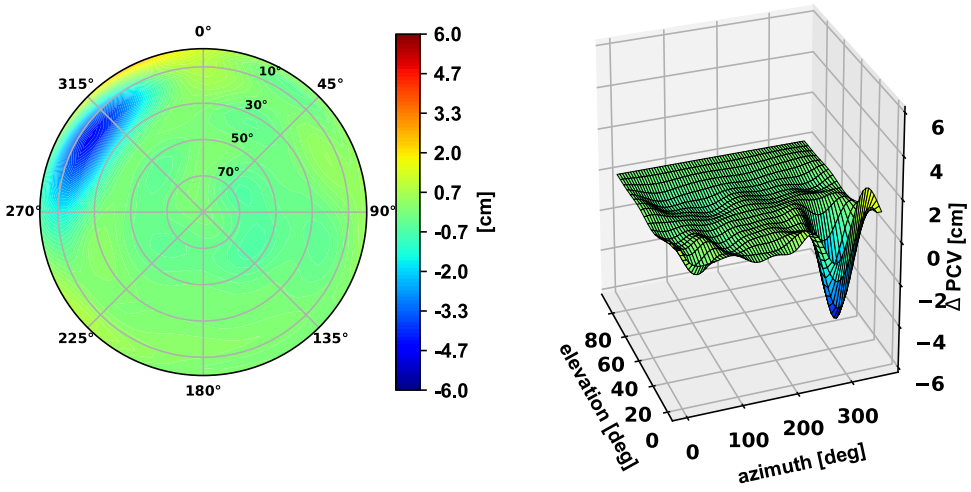


**Fig. 5** Example of L1 PCV difference between a single calibration and the type mean. Polar and 3D plot with respect to azimuth and elevation are reported

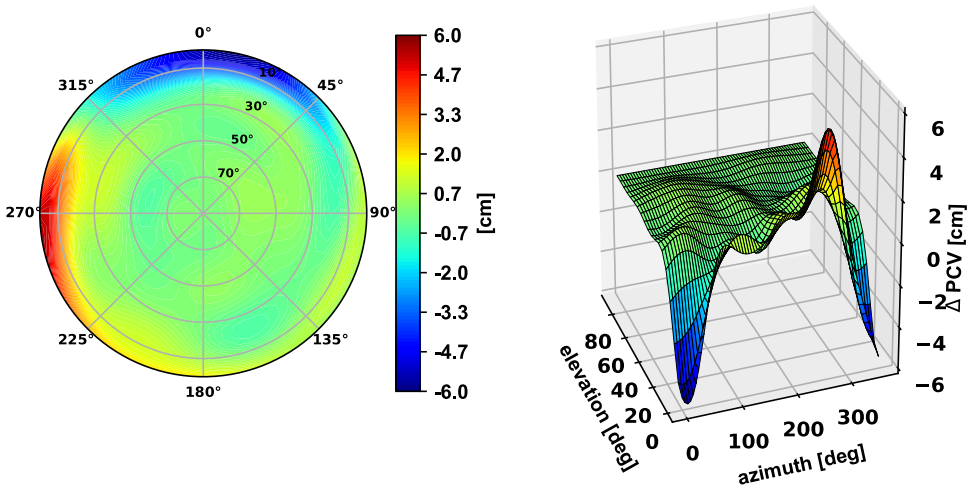


**Fig. 6** Example of L5 PCV difference between a single calibration and the type mean. Polar and 3D plot with respect to azimuth and elevation are reported

between the correction values of a single calibration of 12 h and the type mean correction computed from all calibrations. In the type mean correction, a rigorous adjustment of the individual PCV spherical harmonic expansions with their complete variance–covariance matrix is executed (Wübbena et al. 2006). Some elevation-dependent considerations can be drawn from the comparisons shown in Fig. 5 and Fig. 6. The agreement between the type mean and the individual calibration is better than 5 mm for elevations higher than 20°. For low elevations, significant discrepancies are visible for the azimuth angle ranges mentioned above. This is uncommon for the antenna calibration and may be attributed to the capability to calibrate the smartphone antenna in those particular elevation and azimuth regions.

In addition, for each calibration, the deviation from the type mean is computed for the elevation-dependent PCV and shown in Fig. 7. The PCV differences indicate a deviation of up to 4 mm for L1 and 12 mm for L5, especially for high elevations. These values are larger than usually observed for a rover antenna, i.e., lower than about 4 mm at the horizon and, on average, roughly 1 mm between 15 and 20 deg.

To our knowledge, no published information concerning the Mate20X antenna type and location is available. However, following what was reported by other authors (Banville et al. 2019, Lachapelle and Gratton 2019), the Mate20X is equipped with an omnidirectional linearly polarized antenna. Different factors might contribute to the larger PCV variation of the L5 differences. The L5 tracking performance and the geometry of the constellation of L5-capable satellites are not optimal (because not all the GPS satellites broadcast L5). Furthermore, the Mate20X is equipped with two antennas. Figure 4 shows the location of the estimated antenna centers along with the computed PCO. In Fig. 4, the orientation angle is the azimuth angle introduced in (1). In the calibration setup, the plug of the charger is defined as the North Reference Point (NRP), as shown in Fig. 4. The dimensions reported in Fig. 4 have small uncertainties up to few mm due to

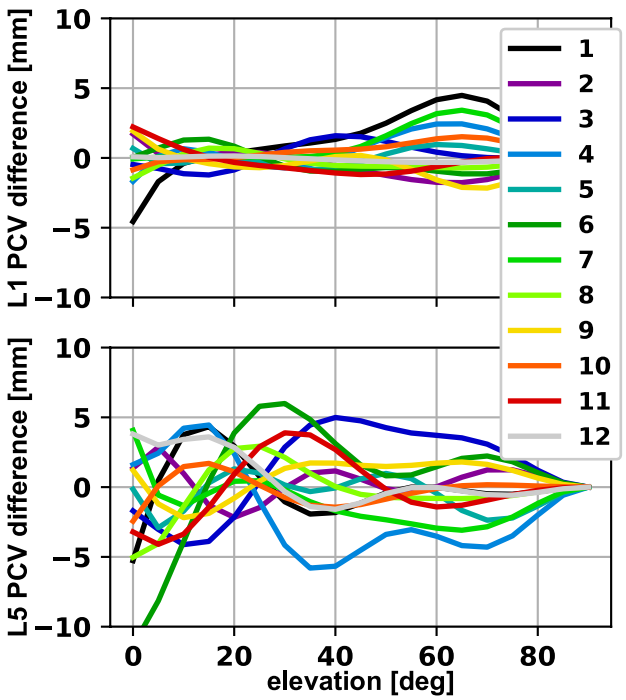


**Fig. 7** Elevation-dependent difference from type mean of the estimated L1 (top row) and L5 (bottom row) PCV computed for each calibration

the precision in positioning the mechanical mount used in the calibration setup. A 1 cm distance (in E-W direction) between the two estimated centers is observed. Besides, the Up component of the PCO is 2 mm and 7 mm for L1 and L5, respectively.

## Application of antenna corrections: positioning results

The PCO and PCV corrections obtained from the calibration have been applied in the positioning algorithm of the GNSMART software to perform smartphone-based positioning. The PCO can be expressed in terms of PCV (Leick et al. 2015). Therefore hereafter, we refer to PCV as the total contribution. The concept behind the employed positioning algorithm is state space modeling (SSM). The main description of the SSM approach can be found in Wübbena and Willgalis (2001), and Wübbena et al. (2001). For the tests, we assume that the two receivers experience the same atmospheric effects. The post-processing algorithm employs an extended Kalman filter (EKF), and an elevation mask of 10 degrees is applied. We achieved ambiguity-fixed epochs with at least four satellites fixed to integers successfully. A satellite has been considered fixed when the ambiguity is fixed to an integer value for two frequencies (i.e., L1 and L5). The ratio test shows values higher than 3, being coherent with what is suggested by Euler and Schaffrin (1991).

To evaluate the impact of the antenna corrections, we carried out tests in different environments. Since the smartphone antenna is susceptible to MP, we collected some measurements on a soccer field (see Fig. 8) to prevent significant ground reflections. The soccer field is located roughly 12 km northwest from a geodetic reference station in Garbsen, Germany. The second environment considered is an open sky environment on the rooftop of the Geo++ building (see Fig. 9) in Garbsen. In the same rooftop conditions and measurements from the same smartphone model, Darugna et al. (2019) already showed that it is not possible to solve ambiguities reliably because of the residual phase biases possibly caused by multipath.

**Fig. 8** Soccer field setup. Left and middle panel: the geodetic receiver has been used to compute the correct reference position of the smartphone. Right panel: the Mate20X has been aligned to geographic north, with the bottom edge eccentric over the reference point (the hole in the piece of cardboard)

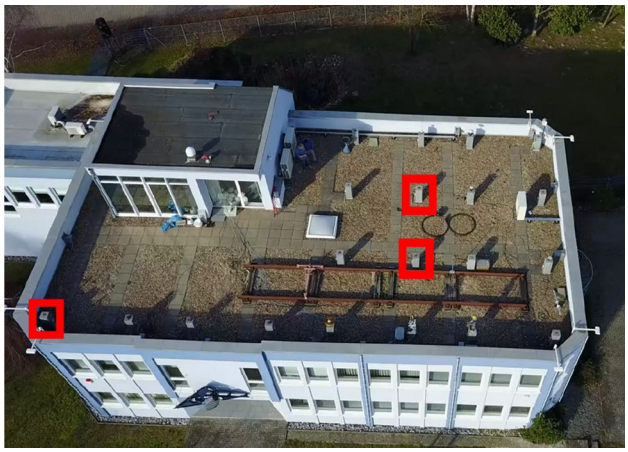

**Fig. 9** Rooftop and multipath environment of the Geo++ building. The pillars within the red squares were chosen as locations for the smartphone tests

## Soccer field test

Figure 8 shows the setup used to perform the measurements. First, we installed a JAVAD geodetic receiver over the center of the pitch. We compute the position of the geodetic receiver using a reference station at the Geo++ building (see Fig. 9), roughly 12 km away. The resulting coordinates are then used as a reference to evaluate the quality of the smartphone-based positioning.

Second, we laid down the Mate20X on the ground orienting the NRP toward north properly and the bottom edge over the reference point coordinated with the geodetic receiver (right panel). We evaluate the performance of the smartphone-based positioning for a local and a remote reference station. The local reference was the geodetic receiver placed over the penalty point, roughly 50 m away, and the remote setup used the stationary reference station at the Geo++ building, 12 km away. About 30 min of measurements was gathered and analyzed.

Figures 10 and 11 show the improvement in positioning that antenna calibration can provide in terms of 2D error. Float and ambiguity resolved results are shown in the two figures, with and without antenna corrections. Figure 10 depicts the 2D positioning error obtained with respect to the local geodetic receiver on the pitch, while Fig. 11 shows the results with respect to the reference station 12 km away. Both figures suggest that the ambiguities were fixed correctly to integers when applying the PCV in both experiments, yielding a 1.5 cm and 3.9 cm 2D error, respectively. The RMSE in the height component is 3.5 cm and 6.1 cm, respectively. The larger values for the remote setup are expected since the atmospheric conditions have a stronger influence on the long baseline. In both cases, the time to fix ambiguities (TTFA) of at least four satellites is lower

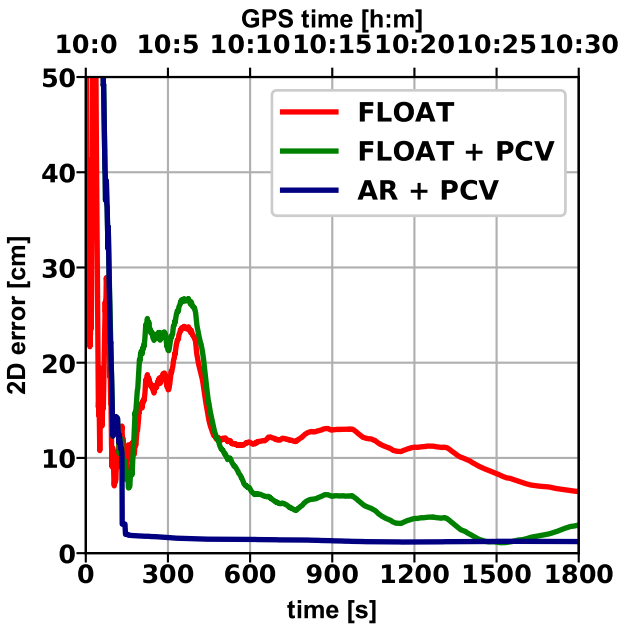


**Fig. 10** Positioning performance in the soccer field: the Mate20X is the rover and the JAVAD receiver about 50 m away is the reference station. The 2D error obtained with and without PCV is compared. Results with float and resolved (AR) ambiguities are reported

than 180 s. While also improving the float solution for most of the time, the primary outcome of the experiment is that

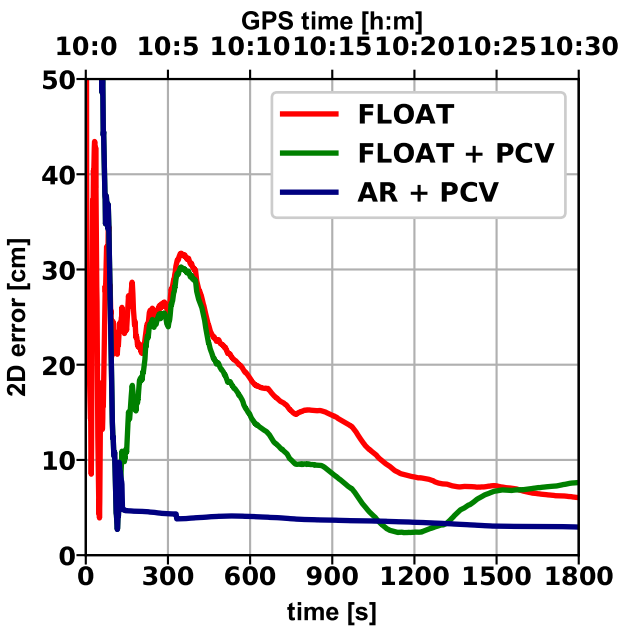


**Fig. 11** Positioning performance in the soccer field: the Mate20X is the rover while the reference station is about 12 km away. The 2D error obtained with and without PCV corrections is compared. Results with float and resolved (AR) ambiguities are reported

the use of antenna corrections opens the possibility to fix ambiguities correctly.

## Rooftop test

To further evaluate the impact of the antenna corrections on ambiguity resolution, a local setup on the roof of the Geo++ building is considered. It is an open sky environment, where several pillars with known coordinates present favorable locations for GNSS testing. The observations of a close (< 10 m) reference station have been exploited using the same positioning approach as in the soccer field test. Here, the repeatability of the performance comparable to the soccer field test case is investigated in more detail.

As shown in Fig. 9, three different pillars were chosen as support for the smartphone (the pillars are squared in red color). The three pillars are differently affected by the small building-block on the top left corner that can be seen in Fig. 9. The smartphone was placed on the surface of the pillar, with the screen facing up and with the NRP correctly oriented toward north. The device lies directly on top of the pillar to remove ground reflections, which can significantly affect the measurements. We collected 35 samples of observations over the three pillars on five different days of the year (DOY) in 2019: 234, 235, 338, 340, 344. In 54% (19 out of 35) of the samples, we achieved a solution with successfully fixed ambiguities.

To understand the underlying reason for the success or failure of fixing, we investigated the satellite geometry and the measured signal strength for the different datasets. A representative comparison between good and bad geometry is reported in the following example. Figures 12 and Fig. 13 show two different observation periods for the phase measurements of GPS single-frequency (L1 or L5 observation is available) and Galileo dual-frequency (both E1 and E5a observations are available). In the first case (Fig. 12), correct ambiguity resolution was not possible, while it was in the second case. Figure 12 shows poor position dilution of precision (PDOP) both for GPS single-frequency and for Galileo dual-frequency, while the same parameters are significantly better in Fig. 13, giving a good indication of why ambiguity resolution was only possible in the latter case. In addition, for the sake of completeness, geometric (G), horizontal (H), and vertical (V) DOP are reported. Also, Figs. 12 and 13 show the number of usable satellites is much lower for the smartphone than the geodetic reference receiver, with numbers as low as 3 or 4 per constellation. This means that there is often not much redundancy in the positioning solution and a single satellite with increased measurement errors can easily make the difference between a reliable and noisy positioning solution. It is worth mentioning that a small PDOP does not assure a successful ambiguity resolution (Wang et al. 2020). However, it is shown that simple considerations about geometry and signal strength provide the user with a fast apriori indication about obtaining a precise solution with smartphone's measurements based only on the geometry.

Figure 14 shows the significant impact of the PCV corrections for the 19 *high-quality* measurements on the different pillars. While for all datasets only float solutions could be achieved without corrections, a centimeter-level fixed positioning was possible when applying them. Figure 14 indicates that, like in the pitch case, the antenna corrections improve the float solution by roughly 1 cm. When applying the antenna corrections, a 2D RMSE of 1.6 cm and an RMSE of 3.8 cm in the height component can be achieved when the ambiguities are successfully fixed to integers (see Fig. 14 and Table 1). The time to fix ambiguities (TTFA) is less than 3 min in 84% of the cases, while all the 19 samples are fixed in less than 6 min, as shown in Fig. 14 looking at the light blue colored lined and summarized in Fig. 15. Moreover, a sub-meter 2D

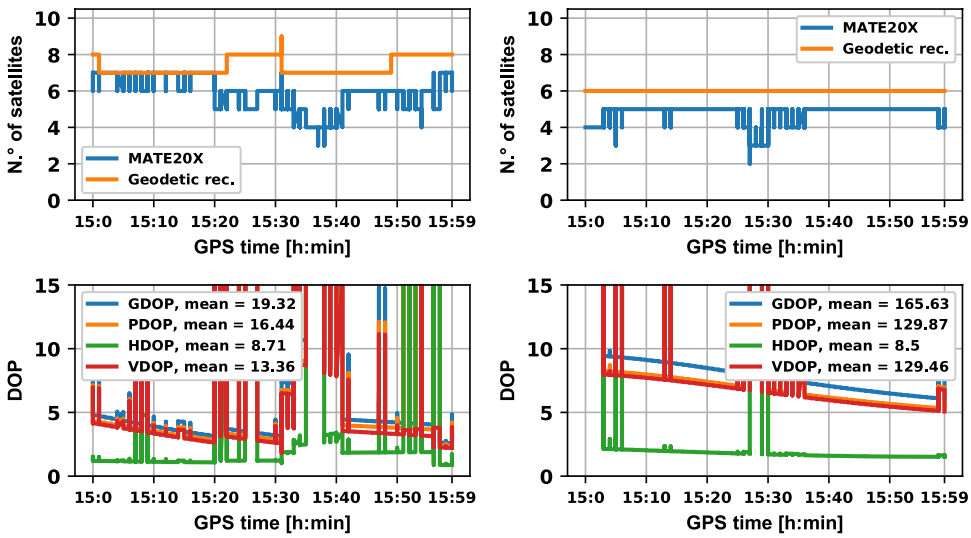


**Fig. 12** Top: number of carrier-phase locked satellites of Mate20X (blue line) and the geodetic receiver (orange line). Bottom: geometric (G), position (P), horizontal (H), and vertical (V) DOP. GPS single-frequency constellation (left) and Galileo dual-frequency (right) during hour 15 (GPS time) at DOY 338. This configuration was not suitable for reliable ambiguity resolution

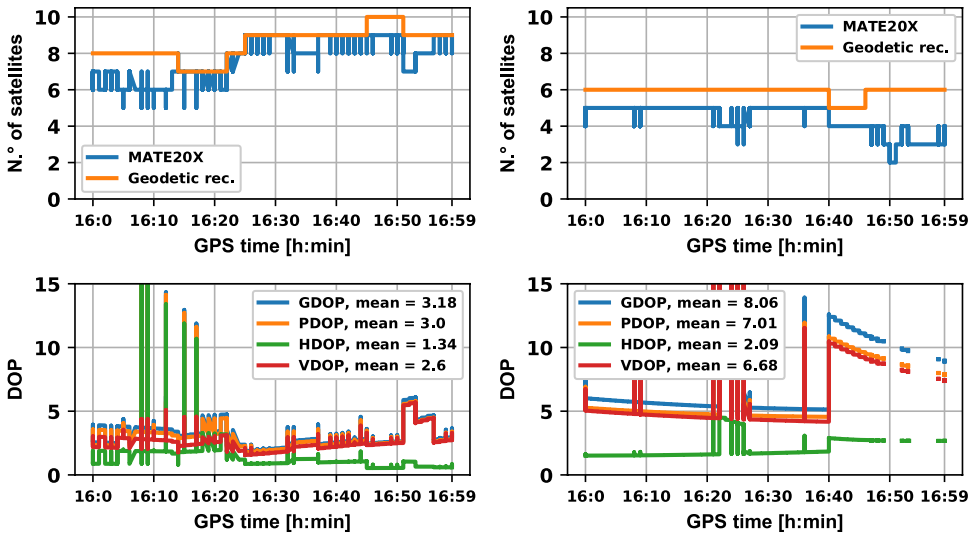


**Fig. 13** Top: number of carrier-phase locked satellites of Mate20X (blue line) and of the geodetic receiver (orange line). Bottom: geometric (G), position (P), horizontal (H), and vertical (V) DOP. GPS single-frequency constellation (left) and Galileo dual-frequency (right) during hour 16 (GPS time) of DOY 338. This configuration was demonstrated suitable for reliable ambiguity resolution

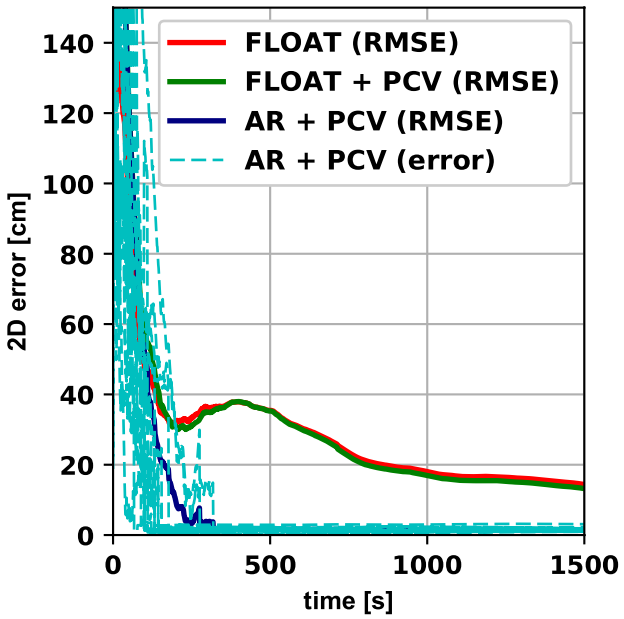


**Fig. 14** Positioning error RMS computed over 19 samples of data collected using the Mate20X lying on a pillar of the Geo++ rooftop. The application of antenna calibration corrections improves the positioning performance and allows ambiguity resolution, resulting in cm-level positioning accuracy. The light blue colored lines show the 2D error of all the 19 samples. The reference station is at a distance lower than 10 m. In the float RMSE, the bump after about 400 s is due to the behavior of some specific samples in which the error was much larger than in the other cases

solution is obtained in about 1 min. Note that, in the soccer-field measurements, a sub-meter 2D error was achieved within a few seconds (Table 1). The difference between the times to reach sub-meter errors can be explained by the much higher code multipath level in the rooftop environment. This leads to bad positioning performance during the first epochs, where the influence of the precise phase measurements is comparably small, and noisy code observations dominate the solution.

In fact, the soccer field test case presents an entirely different multipath environment with respect to the rooftop. The code MP combination is evaluated to assess the multipath level. While in the soccer field, all the absolute values are lower than 2 m, in the roof case, the magnitudes of the MP combination go up to more than 8 m. Besides, the STD of the MP combination is about 0.63 m and 0.57 m for L1 and L5, respectively. In the soccer field, instead, the STD does not exceed 0.43 m and 0.28 m for L1 and L5, respectively.

Figure 16 shows the results in the 16 cases where ambiguity resolution was not possible in terms of 2D error (shaded lines) and 2D RMSE. Although a successful ambiguity resolution was not feasible, a 2D RMSE of 20 cm is achieved in less than 10 min (600 s).

Summarizing, ambiguity resolution with smartphone observations is still challenging because of the constellation geometry of the available phase measurements and the significant impact of the multipath due to the type of antenna used. Nevertheless, it has been demonstrated that, when ground reflections are partially removed, PCV corrections make ambiguity resolution feasible, and cm-level 2D RMSE can be achieved.

## Conclusions

The Geo++ absolute antenna field robot calibration has been used to determine PCV for the Huawei Mate20X smartphone. The calibration has been evaluated over twelve different runs, showing repeatability with elevation-dependent PCV differences lower than 4 mm and 12 mm for L1 and L5,

**Table 1** Time to achieve sub-meter solution (TTSM), time to fix ambiguities (TTFA) with PCV and 2D RMSE with antenna corrections for the setups analyzed

| Setup | Approx. TTSM (s) | TTFA with PCV (average) (s) | 2D RMSE with PCV (cm) |
|---|---|---|---|
| Soccer field ref. station distance 50 m | 5 | 151 | 1.5 |
| Soccer field ref. station distance 12 km | 5 | 166 | 3.9 |
| Rooftop ref. station distance < 10 m | 60 | 142 | 1.6 |

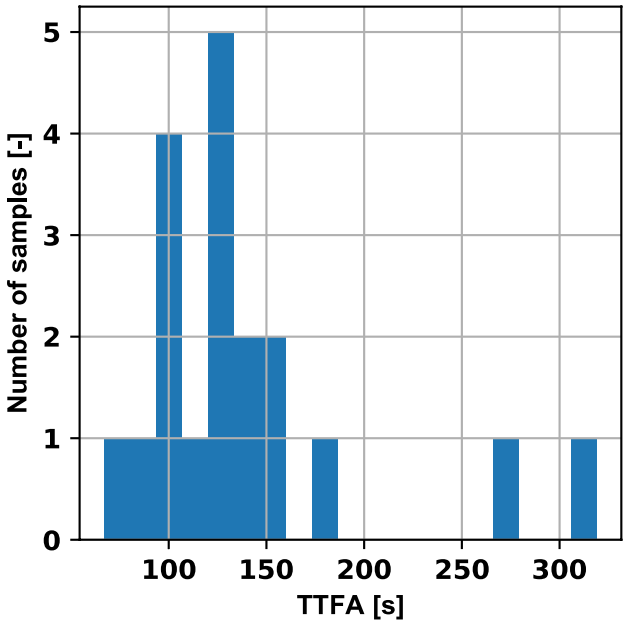


**Fig. 15** Histogram of the TTFA for the 19 samples with successful ambiguity resolution

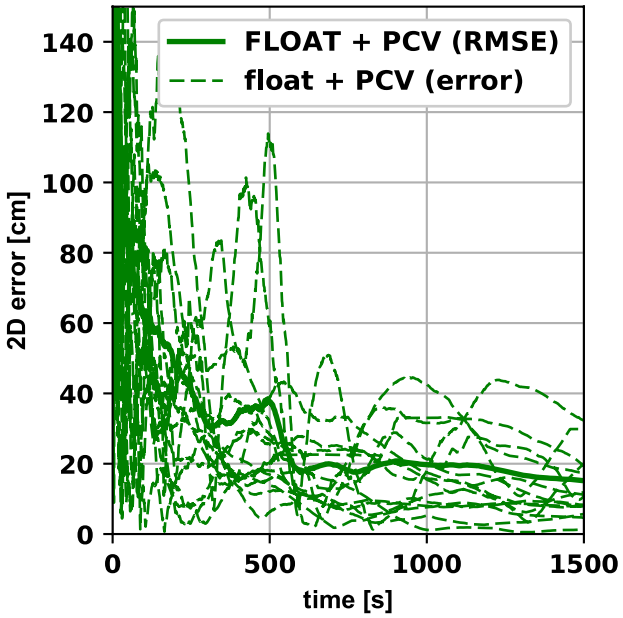


**Fig. 16** Positioning 2D error of 16 samples of data collected using the Mate20X lying on a pillar of the Geo++rooftop. The reference station is at a distance below 10 m. It was not possible to solve ambiguities successfully for the data samples. However, a 2D error of 20 cm is achieved in less than 10 min (600 s). In the RMSE, the bump after about 500 s is due to the behavior of some specific samples in which the error was much larger than in the other cases

respectively. The absolute PCV reach up to about 4 cm with an empirical STD that does not exceed 1 cm.

Different multipath environments have been tested. High-accuracy positioning using the Mate20X and a geodetic receiver has been performed. While without antenna calibration, no reliable ambiguity-fixed solution could be obtained, a 2D error lower than 2 cm (4 cm) has been demonstrated using observations of a reference station 10–50 m (about 12 km) away, when antenna corrections were applied. In both cases, the TTFA is about 3 min. The difference in error magnitude between the two solutions is most likely due to atmospheric effects.

It can be concluded that the calculated PCV are applicable for phone devices, being an asset for smartphone-based positioning with ambiguity resolution. The presented results open a new scientific research direction in high-accuracy positioning using smartphones. Future studies might take advantage of several sensors that are already inside smartphones. A sensor fusion technique can support the antenna correction during moving applications taking care of the smartphone's attitude and enabling the use in different orientations. We believe that expedients to reduce multipath will unveil new GNSS-based semi-professional applications using Android devices.

**Acknowledgment** The investigations were funded in the framework of the research program Training REsearch and Applications Network to Support the Ultimate Real-Time High-Accuracy EGNSS Solution (TREASURE) project. TREASURE has received funding from the European Union's Horizon 2020 research and innovation program under the Marie Skłodowska-Curie grant agreement No 722023. Also, we acknowledge the anonymous reviewers for the valuable contribution to the paper.

**Funding** Open Access funding enabled and organized by Projekt DEAL.

**Data Availability** The data used in this work are not publicly available and belongs to Geo++ GmbH. The data sharing can be agreed with Geo++ GmbH.



## References

Banville S, Lachapelle G, Ghoddousi-Fard R, Gratton P (2019) Automated Processing of Low-Cost GNSS Receiver Data. In: Proc. ION GNSS 2019, Institute of Navigation, Miami, Florida, USA, September 16-20, pp 3636–3652

Bochkati M, Sharma H, Lichtenberger C A, Pany T (2020) Demonstration of Fused RTK (Fixed) + Inertial Positioning Using Android Smartphone Sensors Only. In: Proc. IEEE/ION PLANS, Portland, OR, USA, April 20-23, pp. 1140–1154

Darugna F, Wübbena J, Ito A, Wübbena T, Wübbena G, Schmitz M (2019) RTK and PPP-RTK Using Smartphones: From Short-Baseline to Long-Baseline Applications. In: Proc. ION GNSS 2019, Institute of Navigation, Miami, Florida, USA, September 16-20, pp 3932–3945

Euler HJ, Schaffrin B (1991) On a measure for the discernibility between different ambiguity solutions in the static-kinematic GPS-mode. In: Schwarz KP, Lachapelle G (eds) Kinematic systems in geodesy, surveying, and remote sensing. International association of geodesy symposia, vol 107. Springer, New York

Geng J, Li G (2019) On the feasibility of resolving Android GNSS carrier-phase ambiguities. J Geodesy 93(12):2621–2635

Görres B, Campbell J, Becker M, Siemes M (2006) Absolute calibration of GPS antennas: laboratory results and comparison with field and robot techniques. GPS Solut 10(2):136–145

Humphreys TE, Murrian M, van Diggelen F, Podshivalov S, Pesyna KM (2016) On the feasibility of cm-accurate positioning via a Smartphone's Antenna and GNSS Chip. In: Proc. IEEE/ION PLANS, Savannah, GA, USA, April 11-14, pp 232–242

Kersten T (2014) Bestimmung von Codephasen-Variationen bei GNSS-Empfangsantennen und deren Einfluss auf die Positionierung, Navigation und Zeitübertragung. München: CH Beck. Dissertation, Leibniz University of Hannover

Lachapelle G, Gratton P (2019) GNSS precise point positioning with android smartphones and comparison with high performance receivers. In: Proc. IEEE Int. Conf. on Signal, Information and Data Processing, Chongqing, China, December 11-13

Leick A, Rapoport L, Tatarnikov D (2015) GPS satellite surveying. Wiley, New York

Mader GL (1999) GPS antenna calibration at the national geodetic survey. GPS Solut 3(1):50–58

Massarweh L, Darugna F, Psychas D, Bruno J (2019) Statistical investigation of android GNSS data: case study using Xiaomi Mi 8 dual-frequency raw measurements. In: Proc. ION GNSS 2019, Institute of Navigation, Miami, Florida, USA, September 16-20, pp 3847–3861

Menge F (2003) Zur Kalibrierung der Phasenzentrumsvariationen von GPS-Antennen für die hochpräzise Positionsbestimmung. Dissertation, Leibniz University of Hannover

Netthonglang C, Thongtan T, Satirapod C (2019). GNSS Precise positioning determinations using smartphones. In: 2019 IEEE Asia Pacific Conference on Circuits and Systems (APCCAS), pp 401–404

Pathak V, Thornwall S, Krier M, Rowson S, Poilasne G, Desclos L (2003) Mobile handset system performance comparison of a linearly polarized GPS internal antenna with a circularly polarized antenna. In: IEEE Antennas and Propagation Society International Symposium. Digest. Held in Conjunction with: USNC/CNC/URSI North American Radio Sci. Meeting, vol 3 no 3, pp 666–669

Pesyna Jr KM, Heath Jr RW, Humphreys TE (2014) Centimeter positioning with a smartphone-quality GNSS antenna. In: Proc. ION GNSS 2014, Institute of Navigation, Tampa, Florida, September 8-12, pp 1568–1577

Rothacher M (2001) Comparison of absolute and relative antenna phase center variations. GPS Solut 4(4):55–60

Rothacher M, Schmid R (2010) ANTEX: the antenna exchange format, Version 1.4, 15 Sep 2010. ftp://igs.org/pub/station/general/antex14.txt

Rothacher M, Schaer S, Mervart L, Beutler G (1995) Determination of antenna phase center variations using GPS data. In: Proc. IGS Workshop on Special Topics and New Directions, pp 205–220

Schmitz M, Wübbena G, Boettcher G (2002) Tests of phase center variations of various GPS antennas, and some results. GPS Solut 6(1–2):18–27

Schupler BR, Allshouse RL, Clark TA (1994) Signal characteristics of GPS user antennas. Navigation 41(3):276–296

Teunissen PJ, Montenbruck O (2017) Springer handbook of global navigation satellite system. Springer, Berlin

Wang K, Teunissen PJ, El-Mowafy A (2020) The ADOP and PDOP: two complementary diagnostics for GNSS positioning. J Survey Eng 146(2):04020008

Wanninger L, Heßelbarth A (2020) GNSS code and carrier phase observations of a Huawei P30 smartphone: quality assessment and centimeter-accurate positioning. GPS Solut 24(24):64

Willi D (2019) GNSS receiver synchronisation and antenna calibration. Dissertation, ETH Zurich

Willi D, Lutz S, Brockmann E, Rothacher M (2020) Absolute field calibration for multi-GNSS receiver antennas at ETH Zurich. GPS Solut 24(1):1–15

Wübbena G, Willgalis S (2001) State space approach for precise real time positioning in GPS reference networks. In: Proceedings Int. Symp. on Kinematic Systems in Geodesy, Geomatics and Navigation (KIS2001), pp 5–8

Wübbena G, Schmitz M, Menge F, Seeber G, Völksen C (1997) A new approach for field calibration of absolute GPS antenna phase center variations. Navigation 44(2):247–255

Wübbena G, Schmitz M, Menge F, Böder V, Seeber G (2000) Automated absolute field calibration of GPS antennas in real-time. In: Proc. ION GPS 2000, Institute of Navigation, Salt Lake City, Utah, USA, September 19-22, pp 2512–2522

Wübbena G, Bagge A, Schmitz M (2001) RTK networks based on Geo++ GNSMART–concepts, implementation, results. In: Proc. ION GPS 2001, Institute of Navigation, Salt Lake, UT, USA, September 11-14, pp 368–378

Wübbena G, Schmitz M, Boettcher G, Schumann C (2006) Absolute GNSS antenna calibration with a robot: repeatability of phase variations, calibration of GLONASS and determination of carrier-to-noise pattern. In: Proceedings of the IGS Workshop, pp 8–12

Wu Q, Sun M, Zhou C, Zhang, P (2019) Precise Point Positioning Using Dual-Frequency GNSS Observations on Smartphone. Sensors 19(9)

Xiao B, Wong, H, Wang B, Yeung K L (2019) Effect of the screen to metal-frame smartphone antennas. In 2019 International Workshop on Antenna Technology (iWAT), IEEE, pp 9–32

Zhang X, Tao X, Zhu F, Shi X, Wang F (2018) Quality assessment of GNSS observations from an Android N smartphone and positioning performance analysis using time-differenced filtering approach. GPS Solut 22(3):70



**Francesco Darugna** graduated in aerospace engineering at the University of Padua. Since 2017, he has worked at Geo++ GmbH within the H2020 TREASURE project under a Marie Skłodowska-Curie fellowship and is a Ph.D. candidate at the Leibniz University of Hannover. His research is mainly related to state-space modeling of atmospheric influences and their impact on high-accuracy GNSS positioning, focusing on smartphone-based applications.

**Jannes B. Wübbena** is a managing director at Geo++ GmbH. He graduated in technical physics at the Leibniz University of Hannover, in mathematics at the University of Hagen, and in photonics at the Australian National University. He performed his Ph.D. thesis work on novel atomic clocks at the German National Metrology Laboratory (PTB) in Brunswick. He joined Geo++ in 2014 and is responsible for the development of the core GNSS processing technology.

**Gerhard Wübbena** received a Ph.D. in geodesy from the Universität Hannover. He has worked in the field of GNSS since 1983. In 1990, he founded the company Geo++ GmbH, which develops satellite navigation and positioning software and systems. Among these are the post-processing system GEONAP and the real-time system GNSMART. He is an active member of international working groups of the IGS and RTCM.

**Martin Schmitz** received his Ph.D. in geodesy from the University of Hannover. He has been working in the field of GNSS since 1991, and is involved in research and development of precise GNSS positioning with a focus on RTK networking, antenna and station calibration. He is a member of working groups of the IGS and RTCM.

**Steffen Schön** is a professor for positioning and navigation at IfE since 2006. His research interests are the correction and assessment of systematic errors in GNSS, absolute antenna calibration, receiver clock modeling, and improved stochastic models for GNSS observations based on turbulence theory. He is also currently the spokesman of the DFG research training group integrity and collaboration in dynamic sensor networks, working on interval mathematics for integrity and collaborative navigation.

**André Warneke** received his degrees in geodesy from the University of Hannover. He has been working in the field of GNSS since 2009. Since 2010, he is a support Engineer at Geo++ GmbH, where he is involved in the absolute robot-based field calibration of GNSS antennas.